Preparation of magnetite-silica-cetyltrimethylammonium for phenol removal based on solubility

by Choiril Azmiyawati

Submission date: 18-Jul-2022 11:23AM (UTC+0700)
Submission ID: 1871963847
File name: -2020-Preparation_of_magnetite-silica_cetyltrimethylammonium.pdf (1.16M)
Word count: 4399
Character count: 22558

Research Article

Choiril Azmiyawati*, Endang Sawitri, Parsaoran Siahaan, Adi Darmawan, and Linda Suyati

Preparation of magnetite-silica–cetyltrimethylammonium for phenol removal based on adsolubilization

https://doi.org/10.1515/chem-2020-0040
received September 13, 2018; accepted February 21, 2020

Abstract: In this study, we successfully coated cetyltrimethylammonium–silica on magnetite. The material produced is used to degrade phenol waste in the waters. The effect of the addition of cetyltrimethylammonium bromide (CTAB) on the ability of phenol adsorption was assessed through changes in CTAB concentration of 1, 5, and 10 mM. The results of Fourier-transform infrared spectroscopy explain that CTAB has electrostatic interactions with the silica surface, which is induced by opposite-loaded patches on the opposite surface of silica oxide. The results of the vibrating sample magnetometer show that the magnetite that has been coated by silica–CTA has magnetic properties that are weaker than the initial magnetite, which indicates that the silica–CTA layer has blocked the magnetite. Based on the measurement of the gas sorption analyzer, the largest pore size is in the micro-mesh region, which is between 2 and 6 nm. All magnetite-silica–cetyltrimethylammonium (MS–CTA) showed good adsorption ability of phenol and correlated with the amount of loaded CTAB and admicelle density of the adsorbent. The amount of phenol adsorbed increases proportionately with the increasing density of CTAB admicelles. The maximum phenol adsorption capacity (0.93 mg g^{-1} adsorbent) is achieved by MS–CTA prepared at a CTAB concentration of 10 mM.

Keywords: adsorption, CTAB, magnetite-silica, phenol, admicelles

* **Corresponding author: Choiril Azmiyawati,** Department of Chemistry, Diponegoro University, Semarang, Indonesia, e-mail: choiril.azmiyawati@live.undip.ac.id
Endang Sawitri, Parsaoran Siahaan, Adi Darmawan, Linda Suyati: Department of Chemistry, Diponegoro University, Semarang, Indonesia

1 Introduction

This research focuses on the preparation of adsorbents using magnetite-silica to treat harmful pollutants such as phenol in water. Handling of phenol is essential because the maximum safe concentration is 1 µg L^{-1} [1]; otherwise, phenol can be toxic and harmful to aquatic life and humans. Water treatment technology for phenol degradation is needed to preserve the water quality for human survival and health. Dorigon et al. [2] synthesized mesoporous magnetite-silica–cetyltrimethylammonium bromide (MS–CTAB) for adsorption of dodecylbenzene sulfonate, whereas Ingole et al. [3] used carbon banana peels for adsorption of phenol. Thus, in this study, we synthesized CTA–silica magnetite for use in phenol adsorption.

Magnetite is the material that has the strongest magnetic properties [4] and hence it has the potential for the establishment of the next-generation adsorbents for efficient wastewater treatment in large volumes and rapid separation using an external magnetic field [5]. In this study, magnetite coating with silica aims to support beneficial properties such as chemical safety, thermal properties, and the role of functional groups in protecting the surface of magnetite [6]. The basic principle of this research is the sol–gel reaction in which the transformation of the Si–O–H group into siloxane (Si–O–Si) through a condensation reaction occurs [7]. Sodium silicate (Na_2SiO_3) is hydrolyzed to silicic acid, which is then condensed to produce silanol and siloxane.

The silanol that is obtained as a result of the sol–gel process provides a means to modify the surface of the silica with various functional groups so that it can be adjusted as required. Surface modification of magnetite-silica can be done using surfactants. Surfactants are absorbed on the surface of hydrophilic solids by forming aggregates such as micelles/admicelles when the concentration is above the critical micelle concentration (CMC), i.e., 0.92 mmol L^{-1} [8]. This admicelle interacts

with dissolved ions/nonions in micelles through a mechanism called adsolubilization, including organic substances [9]. Adsolubilization can be used to reduce organic pollutants from wastewater through the absorption or increase of pollutant concentrations on the surface of the adsorbed surfactant aggregates [10].

The surfactant cetyltrimethylammonium bromide (CTAB) can be used for magnetite-silica functionalization. This cationic surfactant attaches to the silica through interaction with the siloxane group [11], and the positive charge on the surfactant head can interact electrostatically with the negative charge of phenolic ions [12,13]. The functionalization of magnetite-silica with CTAB can increase the adsorption capacity of silica to phenols. Monolayers of rod-shaped micelles are formed when the surfactant concentration is equal to or less than the CMC. In contrast, bilayers (admicelles) are formed on the surface of silica magnetite when the surfactant concentration in the solution exceeds CMC [13], as shown in Figure 1.

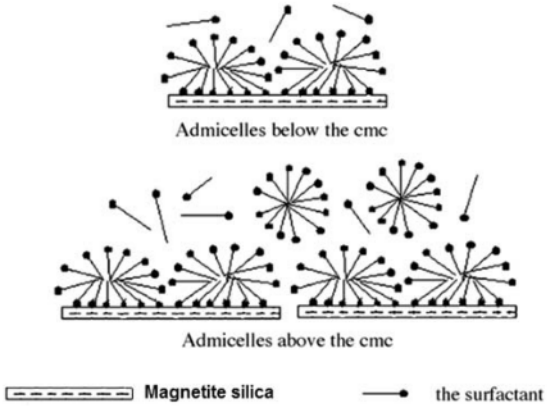

Figure 1: Typical structure of the surfactant aggregates formed on the surface of magnetite-silica [13].

When CTAB was added to the system, ionic interactions between the negative charge of silanol and the positive charge of the amine group on CTAB occur, thus making the carbon chain tail turn away from the silica surface. This implies that the bonding between silica and CTAB is due to electrostatic interaction. The amine peak of CTAB at a wavelength of 1,389 cm^{-1} indicates electrostatic interaction with the negative charge of the silica surface [14].

CTAB has a methylene tail, which gives sharp peaks at 2,924 and 2,850 cm^{-1}. Thus, by monitoring the change in the intensity of the methylene tail, information about the dynamic equilibrium from CTAB absorbed in silica can be obtained. According to Ninness et al. [15] by knowing the frequency and width of the methylene tail peak, which is sensitive to the ratio of the *gauche trans* conformer, information on the structure of the surfactant density can be obtained [15].

Previous studies have shown that the methylene tail in the micelle has a stretching mode with a frequency of 2,924 cm^{-1} and full width at half maximum (FWHM) specific to the characteristic of surfactant tail, typical for CTAB micelles above the oxide surface. The peak intensity of 1,396 cm^{-1} indicates the number of CTAB molecules that bind themselves through electrostatic interactions with the negative charge of the silica surface. The wavelength intensity ratio of 1,396 cm^{-1} as a representation of the number of CTAB molecules adsorbed on the surface of silica through electrostatic interactions compared to wavelength of 2,924 cm^{-1} (the number of CTAB molecules adsorbed due to hydrophobic interactions) is the aggregate percentage of CTAB molecules interacting with the silica surface [16].

Based on the above, synthesis of silica cetyltrimethylammonium magnetite (MS–CTA) as an adsorbent with magnetite obtained from iron sand as a breakthrough technology for effective and inexpensive absorption of phenols was carried out. MS–CTA was characterized by Fourier transform infrared (FTIR) and gas sorption analyzer (GSA) to find the CTAB micelle structure in adsorbents. The magnetic properties of natural magnetite and silica-coated natural magnetite were determined by the vibrating sample magnetometer (VSM). The effect of pH was observed to obtain the optimal application of these adsorbents to adsorb phenol.

2 Experimental

2.1 Reagents and equipment

All reagents were of analytical grade and used immediately after receipt. Reagents used include sodium silicate, hydrochloric acid, CTAB (99%), sodium hydroxide, 1,10-phenanthroline, sodium acetate, hydroxylamine hydrochloride, phenol, sodium nitroprusside, sodium dihydrogen phosphate, and distilled water.

2.2 Synthesis of MS–CTA

Magnetite-silica was prepared according to the previously reported method carried out by Zhao et al. [6] with a few modifications. Magnetite was taken from iron

sand using permanent magnets with a diameter of 15 cm and a thickness of 4 cm. Magnetite was mashed by grinding using a Retsch PM400 Ball mill. The magnetite was then dried using a Memmert oven at 80°C for 4 h and then sieved with a 45 µm sieve. A 10% sodium silicate solution was added dropwise into magnetite. The ratio of the mass of magnetite to Na_2SiO_3 10% was 1:20. To the mixture, 3 M HCl was added to obtain a pH value of ~7. Then, the mixture was stirred for 3 h, with the temperature maintained at 80°C. Finally, the formed silica magnetite was washed thoroughly with distilled water until it was free of chloride ions, and a neutral pH was obtained [6]. The silica magnetite was then heated at 80°C in an oven for 24 h and called MSA_0.

Then in 250 mL of CTAB solution with concentrations of 1, 5, and 10 mmol L^{-1}, 10 g of MSA_0 was added to each. Then, the mixture was stirred with a magnetic stirrer for 24 h and filtered. The solid was washed with distilled water repeatedly until no Br^- ions were detected with no deposits forming in the filtrate by dropping $AgNO_3$. Magnetite-silica–cetyltrimethylammonium (MS–CTA) was then dried at 50°C for 24 h in an oven [17]. Magnetite-silica with the addition of 1, 5, and 10 mmol L^{-1} CTAB solution was represented as MSA_1, MSA_2, and MSA_3.

2.3 Characterization of MS–CTA

The functional group of MS–CTA was analyzed using FTIR. The spectrum of the sample was recorded with a Shimadzu-8201 PC FTIR spectrometer using a KBr disc technique. The spectrum was collected in the range of 400–4,000 cm^{-1}. Surface and pore characteristics were analyzed using the Brunauer–Emmett–Teller method through N_2 adsorption and desorption at liquid N_2 temperature using the Quantachrome GSA Instrument. The concentration of phenol uptake in aqueous solutions before and after adsorption was determined using a UV-Vis spectrophotometer (Genesys 10 Thermo Scientific).

2.4 Determination of influence of pH on phenol adsorption

A total of 15 mL of phenol solution with a concentration of 10 mg L^{-1} was filled into the test tube. The acidity of the phenol solution was adjusted to a pH of 5, 7, 9, or 11 by adding a few drops of 0.1 M HCl or NaOH. Next, 100 mg of MS–CTA was added to the phenol solution. The test tubes were placed into the shaker and rotated at 200 rpm at room temperature with a time variation of 0, 1, 2, 3, 4, 5, and 6 min. The solution was filtered with a fine filter paper, and then the filtrate was analyzed to determine the concentration of the remaining phenol using a UV-Vis spectrophotometer. Adsorption capacity is determined based on equation (1), where initial and time t concentration (mg L^{-1}) is denoted as C_0 and C_t, respectively, m is the adsorbent quantity (g), V is the solution capacity (L), and q_t is the adsorption capacity (mg g^{-1}).

$$q_t = \frac{(C_0 - C_t)\cdot V}{m} \quad (1)$$

Ethical approval: The conducted research is not related to either human or animal use.

3 Results and discussion

3.1 Characteristics of MS–CTA

The FTIR spectra are presented in Figure 2. All spectra show the characteristics of silica spectra. The presence of silica in magnetite is shown by the emergence of a strong SiO_2 peak, which consists of symmetrical stretching of Si–O–Si at 795 cm^{-1}, stretching vibration of Si–OH at 964 cm^{-1}, and asymmetric stretch of Si–O–Si at 1,096 and 1,233 cm^{-1} [18–20]. The presence of broad peaks in the range 3,200–3,750 cm^{-1} and peaks at 1,628 cm^{-1} is related to OH groups in adsorbed silanol and water molecules [21]. The presence of magnetite is characterized by the presence of a Fe–O peak at a wavelength of 471 cm^{-1} [22]. Two intense peaks at around 2,924 and 2,855 cm^{-1}, respectively, are the peaks of the asymmetrical and symmetrical stretching of C–CH_3 from the methylene chain originating from the CTA. This is in line with the emergence of weak peaks in the region of 2,940 to 2,963 cm^{-1} in the solid CTAB spectrum arising from asymmetric stretching of C–CH_3 and symmetrical stretching of N–CH_3 symmetries. The peak at 1,483 cm^{-1} is the asymmetric (CH_3–N^+) deformation mode (δ_{as} CH_3–N^+) of the CTAB head group, and the peak is sensitive to packing density [16]. The appearance of these peaks indicates that CTAB is in magnetite-silica.

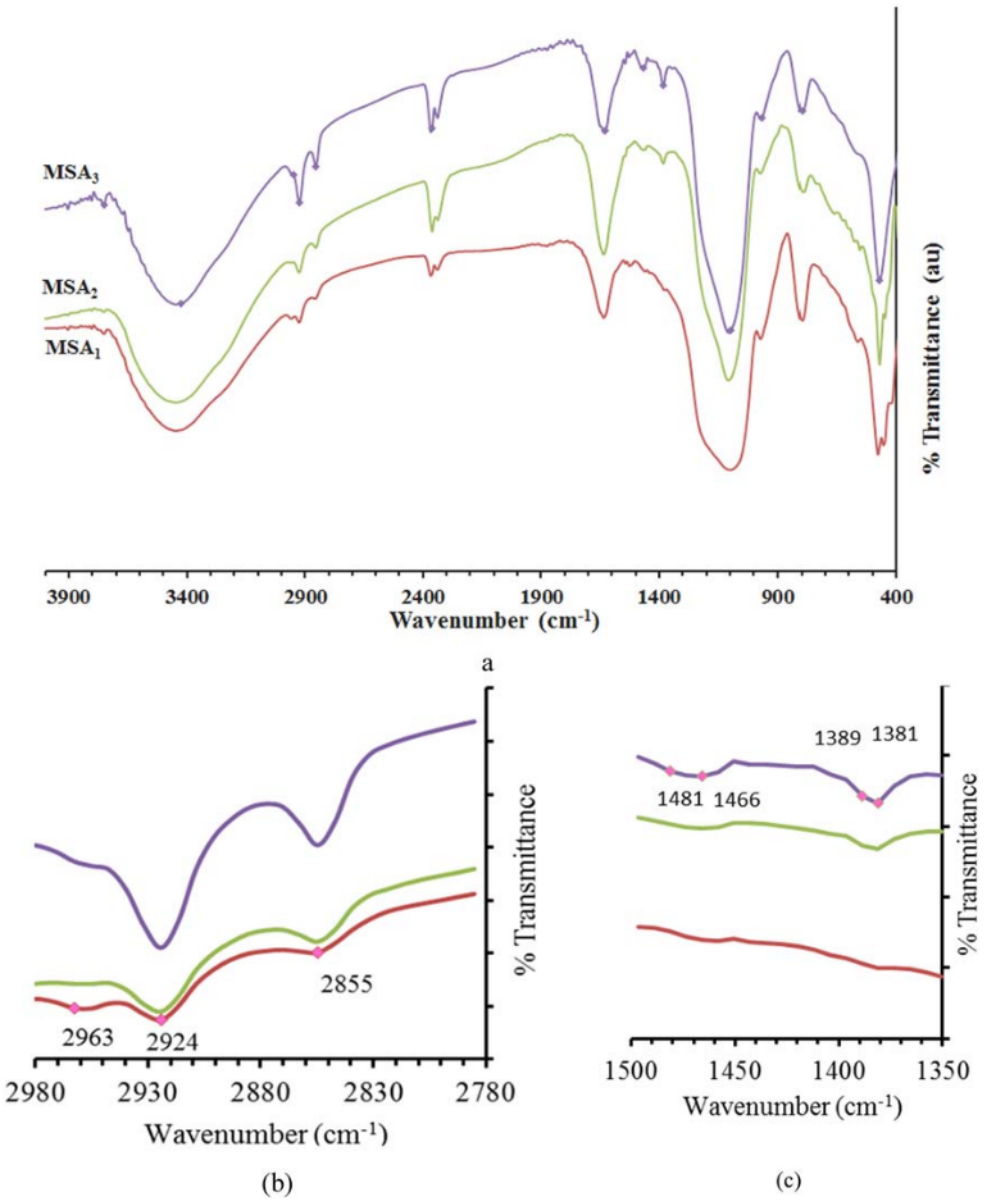

Figure 2: FTIR spectrum result for various MS–CTA: (a) all spectra, (b) inset spectrum of methylene group of CTAB, and (c) inset spectrum of the amine group of CTAB.

All three spectra show similar shapes, which indicate that the chemical environment and functional groups of each material are almost the same.

Figure 2b shows that the methylene stretching mode (2,924 cm^{-1}) has an almost fixed position of frequency and FWHM. Nevertheless, at a wavelength of 1,381 cm^{-1}, significant changes were found, as shown in Figure 2c. The intensity of each vibration is shown in Table 1. The ratio between peak intensities at wavenumbers 1,381 cm^{-1} and 2,854 cm^{-1} is compared. It is seen that the value of the ratio of the peak wavelength changes when the type of material changes.

The CTAB head group attached to the MSA_1 surface appears to be in a normal condition with wavenumbers

Table 1: Vibrational intensity of the functional groups in CTAB

Vibration	Wavenumber (cm^{-1})	Intensity		
		MSA_1	MSA_2	MSA_3
CH_3–N (with silica oxide)	1,381	20.0	28.4	31.6
CH_3–N (free)	1,460	21.9	29.8	33.5
$-CH_2$	2,854	19.0	19.4	23.1
$-CH_2$	2,923	16.5	16.8	19.2
Ratio of 1,381/2,854		1.05	1.46	1.36

1,381 and 1,460 cm^{-1} in the FTIR spectrum. This showed the initial stage of micelle formation in accordance with the characteristics of micelles at a concentration of 1 mM, which is CMC, as shown in Figure 1. The addition of CTAB with concentrations higher than CMC, which were 5 mM MSA_2 and 10 mM in MSA_3, showed slight changes in vibration in CH_2 strains at wavelengths of 2,924 and 2,853 cm^{-1} and significant changes in wavenumbers 1,381 and 1,460 cm^{-1}. This showed an increase in the density of the CTAB aggregate structure attached to silica. Thus, it can be said that the formation of admicelles on MSA_2 and MSA_3 is possible. The magnetism of natural magnetite and CTA–silica magnetite is shown by the results of VSM in Figure 3. The magnetism value for natural magnetite obtained from "Pantai Baru" sand is 45 emu g^{-1},

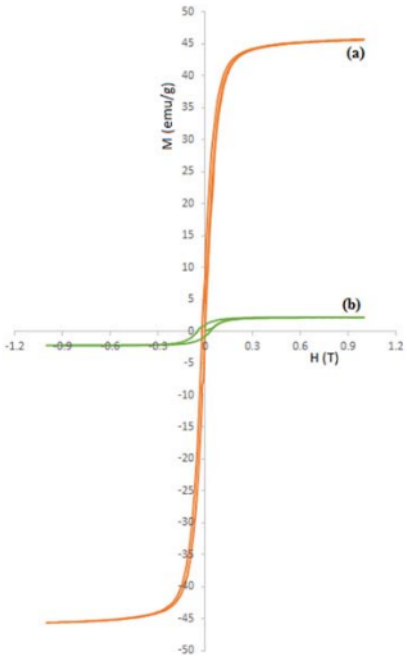

Figure 3: Fe_3O_4 hysteresis curves without (a) and with the addition of silica–CTA (b) using VSM.

whereas for magnetite that has been coated with silica the value is around 2.5 emu g^{-1}. A very significant decline of around 50 times in magnetism was observed. These data indicate that magnetite coatings have been successful.

The nitrogen adsorption–desorption isotherm for MSA_0 is shown in Figure 4a. The figure is a graph of the amount of nitrogen adsorbed according to the relative pressure of P/P_0 of MSA_0. It shows a pattern where there is a rapid increase in the region of low relative pressure (P/P_0), then a slow rise in the middle, and it rises again rapidly as P/P_0 approaches one. The first increase occurred because the absorbed gas molecules create a single layer filling, then in the higher P/P_0 area, the addition of this gas molecule formed a multilayer layer filling where the absorbed gas molecules condensed. The hysteresis loop occurred in the middle region. The isotherm adsorption ensued was a type IV isotherm which is the adsorption from mesoporous solids with a surface area of 337.5 $m^2 g^{-1}$ and a pore size of 8.7 nm, thus supporting the fact that MSA_0 was mesoporous as shown in Figure 4a.

The addition of CTAB to silica magnetite changes the surface character which is marked by the narrowing of the hysteresis loop, which indicates a decrease in surface area. It is estimated that CTAB added to silica fills the inner silica pores so that the silica surface area decreases to 84–87 $m^2 g^{-1}$ and the pore size narrows to 1.8 nm. These results are consistent with studies which state that the more the CTAB is added, the more the surface area of silica decreases [14].

Figure 4b presents a graph of pore size distribution based on the Barret-Joyner-Hallenda (BJH) method. There are two pore regions at 1.8 and 3.7 nm (Figure 4b). These results support the indication that CTAB micellization occurs on the surface of silica at a concentration of 1 mM according to CMC [23]. The effect of adding CTAB causes a decrease in the average pore diameter which experiences an expansion of the distribution at 5.0–6.6 nm, as shown in Figure 4c and d. It appears that the addition of CTAB over silica causes a change in the surface character of the adsorbent. This change was probably due to the addition of micelle density as CTAB concentration increased. Previous research confirmed that change in concentration changes the structure of the micelle into a bilayer with a micellar diameter size of 2.3 nm [24].

3.2 Effect of pH and contact time on phenol adsorption

MS–CTA is expected to be a suitable adsorbent for aromatic compounds such as phenols. Phenol is an undesirable compound in water because of its high level

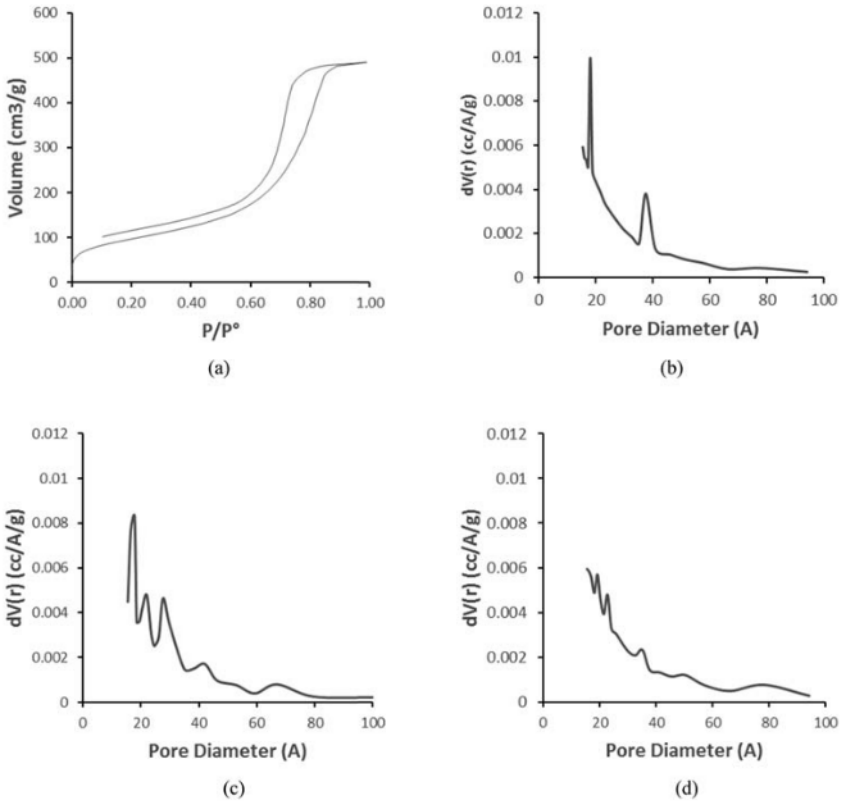

Figure 4: (a) N_2 adsorption–desorption isotherm of MSA_0, (b) pore distribution of MSA_1, (c) pore distribution of MSA_2, and (d) pore distribution of MSA_3.

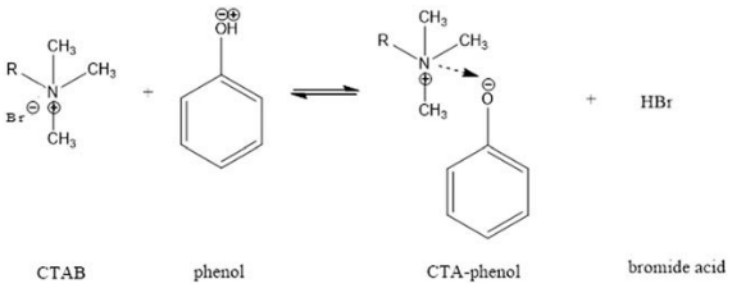

Figure 5: Reaction scheme between CTAB and phenol.

of toxicity and low level of nature. Adsorption of phenols by MSA–CTA is expected to occur based on the mechanism of acid–base reaction. The reaction between phenol and CTAB is estimated to occur as shown in Figure 5, where R is the methylene tail of CTAB.

The concentration of hydrogen ions played an essential role in the phenol adsorption process with magnetite-silica. The effect of pH on phenol capacity is shown in Figure 6. At pH 11, phenol adsorption was very high (up to 78%) when compared to those at pH 5, 7, and 9 (only about 20%). This can be explained by the assumption that CTAB's functionalized silica magnetite surface positively increases the electrochemical interaction between phenol and adsorbent. It is known that

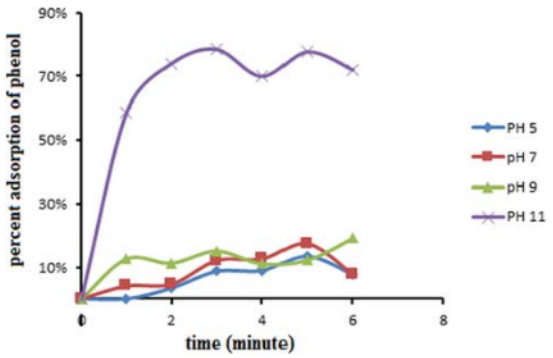

Figure 6: Effect of pH and contact time on percent adsorption of phenol at MSA_3.

the degree of phenol ionization is highly dependent on the pH of the solution. When the pH of the solution is higher than the pK_a value of phenol of +9.92, the phenol will dissociate into phenolic ions ($C_6H_5O^-$). These phenolic ions are easily attracted to the surface of the adsorbent, which tends to be positively charged due to the presence of a CTA head on top of magnetite-silica which acts as a double micelle. Conversely, if the pH is low, the presence of H+ ions will cause an electrostatic repulsion in phenol, which will reduce the adsorption capacity of phenols by CTA which is in silica magnetite [24]. From these data, pH 11 was the optimum condition for the absorption of phenol with MS–CTA.

Figure 6 shows that phenol–CTA interactions are preferred under basic conditions as a consequence of strong electrostatic interactions between negatively charged phenolic ions and positive charges from the cationic surfactant head group of micelles. Although it is in a neutral pH condition, this fact is supported by the opinion of Sabatino *et al.* [12] which states that phenol molecules are specifically located in the outer micelle region under neutral pH conditions (6.70). Conversely, at a more alkaline pH (9.94), the deprotonated phenol molecule ($C_6H_5O^-$) is immersed in the micellar layer of micelles when adsolubilization occurs.

4 Conclusion

Magnetite-silica had been synthesized using CTAB as a surface modification agent. The intensity ratio of the wavelength of 1,396 cm^{-1} as a representation of the number of CTAB molecules adsorbed on the surface of silica through electrostatic interactions compared to the wavelength of 2,924 cm^{-1} (the number of CTAB molecules adsorbed due to hydrophobic interactions) was the aggregate percentage of CTAB molecules that interacted with the surface of silica. When the added CTAB concentration is greater than CMC, micelle/admicelle will form which is evidenced by a narrower and more regular pore size distribution, which is around 1.8 and 3.7 nm. The adsolubilization of phenol in CTAB micelles is profoundly affected by pH, indicating that the phenol–CTAB is present under neutral pH conditions but is most favored under basic conditions as a consequence of the strong electrostatic interaction between the negatively charged phenolic ions and the positive charge of the cationic surfactant head group of micelles.

Acknowledgments: This study was financially supported in part by the Directorate of research and community service, Directorate General Strengthening Research and Development, Ministry of Research, Technology, and Higher Education, Republic of Indonesia through "Competency-based Research" Program, Number: 101-66/UN7.P4.3/PP/2018, 5 February 2018.

Conflict of interest: The authors declare no conflict of interest.

References

[1] Peraturan Pemerintah Republik Indonesia Nomor 82 Tahun 2001 Tentang Pengelolaan Kualitas Air dan Pengendalian Pencemaran Air, in Pemerintah Republik Indonesia, Jakarta; 2001. p. 1–28.
[2] Dorigon L, Ruiz de Almeida da Frota JP, Kreutz JC, Mello Giona R, Pereira Moisés M, Bail A. Synthesis and characterization of mesoporous silica-coated magnetite containing cetyltrimethylammonium bromide and evaluation on the adsorption of sodium dodecylbenzenesulfonate. Appl Surf 2017;420:954–62.
[3] Ingole RS, Lataye DH, Dhorabe PT. Adsorption of phenol onto banana peels activated carbon. KSCE J Civil Eng. 2017;21(1):100–10. doi: 10.1007/s12205-016-0101-9.
[4] Teja AS, Koh P-Y. Synthesis, properties, and applications of magnetic iron oxide nanoparticles. Prog Cryst Growth Charact Mater. 2009;55(1):22–45. doi: 10.1016/j.pcrysgrow.2008.08.003.
[5] Reddy DHK, Yun Y-S. Spinel ferrite magnetic adsorbents: alternative future materials for water purification? Coord Chem Rev. 2016;315:90–111.
[6] Zhao X, Shi Y, Wang T, Cai Y, Jiang G. Preparation of silica-magnetite nanoparticle mixed hemimicelle sorbents for extraction of several typical phenolic compounds from environmental water samples. J Chromatogr A. 2008;1188(2):140–7. doi: 10.1016/j.chroma.2008.02.069.

[7] Essien ER, Olaniyi OA, Adams LA, Shaibu RO. Sol-gel-derived porous silica: economic synthesis and characterization. J Miner Mater Charact Eng. 2012;11(10):976–81. doi: 10.4236/jmmce.2012.1110098.

[8] Woods DA, Petkov J, Bain CD. Surfactant adsorption kinetics by total internal reflection Raman spectroscopy. 2. CTAB and triton X-100 mixtures on silica. J Phys Chem B. 2011;115(22):7353–63. doi: 10.1021/jp201340j.

[9] Koner S, Pal A, Adak A. Utilization of silica gel waste for adsorption of cationic surfactant and adsolubilization of organics from textile wastewater: a case study. Desalination. 2011;276(1):142–7. doi: 10.1016/j.desal.2011.03.035.

[10] Okamoto N, Tomokazu Yoshimura T, Esumi K. Effect of pH on adsolubilization of single and binary organic solutes into a cationic hydrocarbon surfactant adsorbed layer on silica. J Colloid Interface Sci. 2004;275(2):612–7. doi: 10.1016/j.jcis.2004.02.062.

[11] Lüderitz LAC, Klitzing R. Interaction forces between silica surfaces in cationic surfactant solutions: an atomic force microscopy study. J Colloid Interface Sci. 2013;(402):19–26. doi: 10.1016/j.jcis.2012.11.007.

[12] Sabatino P, Szczygiel A, Sinnaeve D, Hakimhashemi M, Saveyn H, Martins JC, et al. NMR study of the influence of pH on phenol sorption in cationic CTAB micellar solutions. Colloids Surf A. 2010;370(1):42–8. doi: 10.1016/j.colsurfa.2010.08.042.

[13] Sun L, Zhang C, Chen L, Liu J, Jin H, Xu H, et al. Preparation of alumina-coated magnetite nanoparticle for extraction of trimethoprim from environmental water samples based on mixed hemimicelles solid-phase extraction. Anal. Chim. Acta. 2009;638(2):162–8. doi: 10.1016/j.aca.2009.02.039.

[14] Ma X-K, Lee N-H, Oh H-J, Kim J-W, Rhee C-K, Park K-S, et al. Surface modification and characterization of highly dispersed silica nanoparticles by a cationic surfactant. Colloids Surf A. 2010;358(1):172–6. doi: 10.1016/j.colsurfa.2010.01.051.

[15] Ninness BJ, Bousfield DW, Tripp CP. The importance of adsorbed cationic surfactant structure in dictating the subsequent interaction of anionic surfactants and polyelectrolytes with pigment surfaces. Colloids Surf A. 2002;203(1):21–36. doi: 10.1016/S0927-7757(01)01088-3.

[16] Li H. IR studies of the interaction of surfactants and polyelectrolytes adsorbed on TiO_2 particles. Orono, Maine: The University of Maine; 2004.

[17] Mahvi AH, Vosoughi M, Mohammadi MJ, Asadi A, Hashemzadeh B, Zahedi A, et al. Sodium dodecyl sulfate modified-zeolite as a promising adsorbent for the removal of natural organic matter from aqueous environments, Health Scope. 2016;5(1):e29966. doi: 10.17795/jhealscope-29966.

[18] Saputra RE, Astuti Y, Darmawan A. Hydrophobicity of silica thin films: the deconvolution and interpretation by Fourier-transform infrared spectroscopy. Spectrochim Acta A Mol Biomol Spectrosc. 2018 Jun;199:12–20.

[19] Darmawan A, Motuzas J, Smart S, Julbe A, Diniz da Costa JC. Gas permeation redox effect of binary iron oxide/cobalt oxide silica membranes. Separ Purif Technol. 2016;171:248–55.

[20] Darmawan A, Utari R, Saputra RE, Suhartana, Astuti Y. Synthesis and characterization of hydrophobic silica thin layer derived from methyltrimethoxysilane (MTMS). IOP Conf Series Mater Sci Eng. 2017;299:012041.

[21] Araghi SH, Entezari MH, Chamsaz M. Modification of mesoporous silica magnetite nanoparticles by 3-amino-propyltriethoxysilane for the removal of Cr(VI) from aqueous solution. Microporous Mesoporous Mater. 2015;[illegible]101–11.

[22] Faivre D, Oxides I. From nature to applications. Wiley-VCH Verlag GmbH & Co. KGaA; 2016. doi: 10.1002/9783527691395.

[23] Smått J-H, Schunk S, Lindén M. Versatile double-templating synthesis route to silica monoliths exhibiting a multimodal hierarchical porosity. Chem Mater. 2003;15(12):2354–61. doi: 10.1021/cm0213422.

[24] Adriano da Silva J, Dias RP, da Hora GC, Soares TA, Meneghetti MR. Molecular dynamics simulations of cetyl-trimethylammonium bromide (CTAB) micelles and their interactions with a gold surface in aqueous solution. J Braz Chem Soc. 2018;29:191–9.

Preparation of magnetite-silica-cetyltrimethylammonium for phenol removal based on solubility

ORIGINALITY REPORT

13%	11%	9%	3%
SIMILARITY INDEX	INTERNET SOURCES	PUBLICATIONS	STUDENT PAPERS

PRIMARY SOURCES

1	digitalcommons.library.umaine.edu Internet Source	1%
2	revistas.unimilitar.edu.co Internet Source	1%
3	www.hindawi.com Internet Source	1%
4	academic.hep.com.cn Internet Source	1%
5	academictree.org Internet Source	1%
6	Haiyan Li, Carl P. Tripp. " Spectroscopic Identification and Dynamics of Adsorbed Cetyltrimethylammonium Bromide Structures on TiO Surfaces ", Langmuir, 2002 Publication	1%
7	revistas.unal.edu.co Internet Source	1%
8	ir.unilag.edu.ng Internet Source	

		1 %
9	shura.shu.ac.uk Internet Source	1 %
10	"Handbook of Sol-Gel Science and Technology", Springer Science and Business Media LLC, 2018 Publication	<1 %
11	Submitted to Universiteit van Amsterdam Student Paper	<1 %
12	Yaswant Kumar Pankaj, Mahesh Jagadale Vasantrao, Nilmani Prakash, Raj Kumar Jat, Rajesh Kumar, Vinay Kumar, Pankaj Kumar. "RETRACTED: Characterization of wheat (Triticum aestivum L.) genotypes unraveled by molecular markers considering heat stress", Open Agriculture, 2019 Publication	<1 %
13	www.jett.dormaj.com Internet Source	<1 %
14	Xiang Zhu, Shuhao An, Yu Liu, Jun Hu et al. "Efficient removal of organic dye pollutants using covalent organic frameworks", AIChE Journal, 2017 Publication	<1 %
15	annals.org Internet Source	<1 %

16	123dok.com Internet Source	<1 %
17	"Dissertation titles", Polymer Contents, 2005 Publication	<1 %
18	cjche.cip.com.cn Internet Source	<1 %
19	worldwidescience.org Internet Source	<1 %
20	www.science.gov Internet Source	<1 %
21	Mohan Rao, P.K.. "The influence of hydrogen ion concentration on radiation-induced damage in barley", Radiation Botany, 1965 Publication	<1 %
22	www.ncshm.re.kr Internet Source	<1 %
23	crossmark.crossref.org Internet Source	<1 %
24	Hongmin Wang, Chan Wang, Shengyang Tao, Jieshan Qiu, Yongxian Yu, Minfen Gu. "Biomimetic Preparation of Hybrid Porous Adsorbents for Efficiently Purifying Complex Wastewater", ACS Sustainable Chemistry & Engineering, 2016 Publication	<1 %

25	arxiv.org Internet Source	<1%
26	link.springer.com Internet Source	<1%
27	Tommy Martho Palapa, Alfonds Andrew Maramis. "Heavy Metals in Water of Stream Near an Amalgamation Tailing Ponds in Talawaan – Tatelu Gold Mining, North Sulawesi, Indonesia", Procedia Chemistry, 2015 Publication	<1%
28	discovery.researcher.life Internet Source	<1%
29	Maryam Arabi, Mehrorang Ghaedi, Abbas Ostovan. "Development of a Lower Toxic Approach Based on Green Synthesis of Water-Compatible Molecularly Imprinted Nanoparticles for the Extraction of Hydrochlorothiazide from Human Urine", ACS Sustainable Chemistry & Engineering, 2017 Publication	<1%
30	Tsai, W.T.. "Adsorption of bisphenol-A from aqueous solution onto minerals and carbon adsorbents", Journal of Hazardous Materials, 20060630 Publication	<1%
	repo-dosen.ulm.ac.id	

31	Internet Source	<1%
32	shareok.org Internet Source	<1%
33	Ayoob, S.. "Performance evaluation of modified calcined bauxite in the sorptive removal of arsenic(III) from aqueous environment", Colloids and Surfaces A: Physicochemical and Engineering Aspects, 20070201 Publication	<1%

Exclude quotes	Off	Exclude matches	Off
Exclude bibliography	Off		